Measurement of the reaction $\pi^- p \rightarrow \pi^+ \pi^- n$ on a transversely polarized target at 17 GeV

H. Becker, W. Blum, V. Chabaud, H. de Groot, H. Dietl, J. Gallivan,
B. Gottschalk, G. Hentschel, B. Hyams, E. Lorenz, G. Lütjens,
G. Lutz, W. Männer, B. Niczyporuk, D. Notz, T. Papadopoulou,
R. Richter, K. Rybicki, U. Stierlin, B. Stringfellow,
M. Turala, P. Weilhammer and A. Zalewska.

CERN-Munich Collaboration

ABSTRACT

Preliminary results of the measurement of the reaction $\pi^- p_\uparrow \rightarrow \pi^+ \pi^- n$ at 17.2 GeV are presented. Strong nucleon polarization effects are observed in the low $|t|$ range where one pion exchange was supposed to dominate. They are due to the presence of s-channel nucleon spin nonflip amplitudes for unnatural parity exchange which correspond to the exchange of an object with the quantum numbers of the A_1.

A model independent amplitude analysis on the data is performed and the results are compared with a model fit to the data adding A_1 and A_2 exchange to the "poor man's absorption " model.

Submitted to the XVIII International Conference on High Energy Physics at Tbilisi (July 15-21, 1976).

INTRODUCTION

The reaction $\pi^- p \rightarrow \pi^+\pi^- n$ has been measured quite precisely already on pure hydrogen targets in several high statistics experiments[1,2]. Data from these experiments have been widely used for the study of π-π scattering[3,4,5] and for the study of resonance production[6,7] in general. Theoretical assumptions had to be introduced in these analyses as no nucleon polarization measurements existed at that time. An absence of A_1-type exchange was assumed in all these analyses. Here we mean that the s-channel helicity amplitudes were supposed to be purely of spin flip type for the unnatural parity exchange.

The present experiment was carried out to test these assumptions and more generally to allow a model independent amplitude analysis of the reaction. The preliminary results described in this report show strong nucleon polarization effects at low four-momentum transfer. This clearly demonstrates the presence of amplitudes corresponding to the exchange of an object with the quantum numbers of the A_1.

In the following we start with some definitions of kinematic variables, amplitudes and moments of the angular distribution allowing later on a clear presentation of our results. A short paragraph deals with apparatus, measurement and method of data reconstruction. After presenting some features of the raw data sample we show the moments of the angular distribution and determine the transversity amplitudes from our data in the ρ mass region.

DEFINITIONS, MOMENTS AND AMPLITUDES

At fixed beam momentum the reaction is completely defined by 5 variables (fig.1). These are $m_{\pi\pi}$ the mass of the pion pair, t the four momentum transfer to the nucleon, ψ the angle between the normal to the production plane and the (transverse) proton polarization $\vec{P}$, and θ,ϕ the decay angles of the π^- in the $\pi^+\pi^-$ rest system (s or t channel helicity frame).

Due to parity conservation (and spin $\frac{1}{2}$ of the nucleus) the angular distribution (fixed $s,t,m_{\pi\pi}$) is of the general form

$$I(\psi,\cos\theta,\phi) = I_0(\cos\theta,\phi) + P\cos\psi I_1(\cos\theta,\phi) + P\sin\psi I_2(\cos\theta,\phi)$$

with I_0, I_1 symmetric; I_2 antisymmetric in ϕ.
Consequently the angular distribution can be represented by its moments $\langle \mathrm{Re}\, Y^{\ell}_{m}(\Omega)\rangle$, $\langle \cos\psi \mathrm{Re}\, Y^{\ell}_{m}(\Omega)\rangle$ and $\langle \sin\psi \mathrm{Im}\, Y^{\ell}_{m}(\Omega)\rangle$.

A complete description of the reaction is given by the set of helicity amplitudes $\langle jm\chi|T|\lambda\rangle$

$$N^{j}_{m} = \langle j,m,+|T|+\rangle = (-1)^{m+1}\langle j,-m,-|T|-\rangle$$

$$F^{j}_{m} = \langle j,m,+|T|-\rangle = (-1)^{m}\langle j,-m,-|T|+\rangle$$

(j,m angular momentum state of the π pair, χ,λ helicities of neutron and proton). Alternately one uses combinations of amplitudes

$${}^{u}n^{j}_{m} = \frac{1}{\sqrt{2}}(N^{j}_{m} - (-1)^{m}\cdot N^{j}_{-m}) \text{ for } m \neq 0 \qquad n^{j}_{0} = N^{j}_{0}$$

$${}^{N}n^{j}_{m} = \frac{1}{\sqrt{2}}(N^{j}_{m} + (-1)^{m}\cdot N^{j}_{-m})$$

(similar equations for spin flip amplitudes) corresponding to unnatural and natural spin parity exchange.

These amplitudes cannot be determined uniquely by the experiment - for this purpose a measurement of the neutron polarization would be necessary - however two sets of nucleon transversity amplitudes g and h

$${}^{u}g^{j}_{m} = \frac{1}{\sqrt{2}}({}^{u}n^{j}_{m} + i\ {}^{u}f^{j}_{m}) \qquad {}^{N}g^{j}_{m} = \frac{1}{\sqrt{2}}({}^{N}n^{j}_{m} - i\ {}^{N}f^{j}_{m})$$

$${}^{u}h^{j}_{m} = \frac{1}{\sqrt{2}}({}^{u}n^{j}_{m} - i\ {}^{u}f^{j}_{m}) \qquad {}^{N}h^{j}_{m} = \frac{1}{\sqrt{2}}({}^{N}n^{j}_{m} + i\ {}^{N}f^{j}_{m})$$

can be determined.

An illustration of these properties (which hold for arbitrary $\pi\pi$ spin combinations) can be seen from Table 1, where the moments of the angular distribution are given in terms of amplitudes for the case of S- and P-waves only. It is valid for both s and t channel amplitudes as long as the nucleon helicities are defined in the s-channel system. No products of g and h appear in the table, therefore the relative phase between the sets of g and h amplitudes is not measured.

APPARATUS, MEASUREMENT, DATA RECONSTRUCTION AND STATISTICS

The experiment was done with the CERN-Munich spectrometer at the CERN PS (fig.2). A butanol target (length = 10 cm, Ø = 2 cm, average polarization 68%) inside of a 25 kG homogeneous field replaced the hydrogen target used in our earlier experiment[1]). The butanol target could be replaced by a hydrogen target of identical shape in order to study background problems and for cross section normalization studies. A tungsten scintillator shower counter system between the pole faces of the target magnet suppressed background from events with addditional π^0's or charged particles. Proportional chambers directly in front and behind the target in the magnetic field allowed a good vertex determination. An array of 36 scintillation counters mounted parallel to the beam direction around the target was used to measure the angle of the recoil proton in the elastic scattering calibration runs. A beam spectrometer allowed determination of momentum and direction of the incident particle.

The rest of the spectrometer as well as the trigger were essentially identical to that of the earlier experiment[1]).

The presence of Carbon and Oxygen in Butanol (C_4H_9OH) leads to some problems in this experiment where the outgoing neutron remains undetected and a separation of events off hydrogen (as done in four constraint reactions) is not possible. (The widening of the missing mass distribution due to the Fermi motion is negligible compared to the missing mass resolution). We therefore measure in this experiment only the polarization dependent part of the cross section $\frac{d\sigma}{dmdt}\langle\cos\psi \mathrm{Re}\, Y_m^\ell\rangle$ and $\frac{d\sigma}{dmdt}\langle\sin\psi \mathrm{Im}\, Y_m^\ell\rangle$ since the unpolarized Carbon does not contribute to it. For the amplitude analysis the result of this experiment is combined with the results of the hydrogen experiment taken at the same beam energy of 17.2 GeV.

We emphasize that the moments $\langle \cos\psi \mathrm{Re}\, Y_m^\ell \rangle$ and $\langle \sin\psi \mathrm{Im}\, Y_m^\ell \rangle$ could be determined already with one direction of the proton polarization since our apparatus covers a large solid angle. Moreover the results for both polarization directions are consistent (changing of polarization was done once a day by a small change of the klystron frequency only, leaving the spectrometer, and therefore its acceptance unchanged). The final acceptance corrected moments were averaged for the two polarization directions.

The method of acceptance correction was a generalization of the "method of moments" described in ref.[1]).

A total of $1.0 \cdot 10^6$ $\pi^+\pi^- n$ events off butanol with $MM^2 < 1.3$ GeV^2 have been obtained. Roughly one third of these events are off hydrogen (with 68% polarization). Taking into account the unpolarized background the experiment is statistically equivalent to a hypothetical experiment with 60 000 events on pure 100% polarized protons (compared to 300 000 events in our previous hydrogen experiment[1]).

RAW DATA SPECTRA

The missing mass spectra of events from butanol (calculated under the assumption that the process occurs on hydrogen at rest) show a significant enhancement in the MM^2 above the neutron peak (fig.3). This enhancement is not seen in events on the hydrogen target (taken in the same experiment under identical conditions) which have the expected almost symmetric distribution around the neutron mass. This background is independent of $m_{\pi\pi}$ but varies with t and is strongest for low $|t|$ values. It is most probably due to complex interactions on Carbon in which the excited nuclei decay in a mode not detected by our veto counter system (for example by emitting 2 neutrons). Support for this assumption comes from the fact that we do not find polarization for these high MM^2 events.

Strong polarization effects are already seen in the data before applying acceptance correction when we compare distributions of events where the only change is the polarization direction (apparatus including magnetic fields was otherwise identical). The change in distribution in ψ, the angle between normal to production plane and the positive polarization direction, for all events is shown in fig. 4. (4a and 4b would be identical if no nucleon polarization effects were present).

RESULTS

One interesting result of this experiment is the fact that the angular distribution of the events off Carbon is indistinguishable from that of hydrogen. This is shown in fig.5 where some normalized $\langle \mathrm{Re}\, Y_0^\ell \rangle$ moments are given as a function of $m_{\pi\pi}$ for both hydrogen and Butanol. All details including the K-K threshold behaviour are exactly reproduced.

We may consider this result as an argument in favour of the factorization into production and decay amplitudes. Simultaneously we treat this result as a test of our methods of analysis which give identical results for two cases of significantly different geometry. It also indicates the possibility of studying resonance production off complex nuclei.

The mass dependence of $\frac{d\sigma}{dmdt}\langle Y_0^\ell \rangle$ and $\frac{d\sigma}{dmdt}\langle \cos\psi Y_0^\ell \rangle$ for 100% polarized hydrogen ($0.01 < |t| < 0.2$) is shown in fig. 6 (results of hydrogen[1]) and butanol experiment combined). There is still a preliminary uncertainty of 25% in the relative normalization of the two experiments.

A most interesting observation is the presence of strong polarization effects (at the ρ mass the $2\langle \cos\psi Y_0^0 \rangle / \langle Y_0^0 \rangle$ is -0.35, the maximum possible value being -1) in the low t region. Let us remind ourselves that according to general belief this region should be dominated by π-exchange and therefore should exhibit little or no polarization effects. An inspection of table 1 shows that the polarization dependent moments $\langle \cos\psi \mathrm{Re}\, Y_m^\ell \rangle$ are due to the simultaneous presence of spin flip and nonflip amplitudes of equal naturality (unnatural in this t range). The $\langle \sin\psi \mathrm{Im}\, Y^{\ell}_{m} \rangle$ moments are compatible with zero for this t range. The t-dependence of the cross section $\frac{d\sigma}{dt}$ and the normalized moments $\langle \cos\psi Y^{0}_{0} \rangle$ in the ρ mass region are shown in fig.7

The moments $\langle \cos\psi \mathrm{Re} Y^{\ell}_{m} \rangle$ exhibit (with opposite sign) the same structure as $\langle \mathrm{Re} Y^{\ell}_{m} \rangle$. One has to a good approximation $\langle \cos\psi \mathrm{Re} Y^{\ell}_{m} \rangle / \langle \mathrm{Re} Y^{\ell}_{m} \rangle$ constant. This relation could be deduced from our earlier considerations on the density matrix[7]) in the ρ region. From the vanishing of an eigenvalue of the density matrix one obtains the relation: ${}^{u}n^{j}_{m} = c \cdot {}^{u}f^{j}_{m}$ with complex c independent of j,m. This in turn leads to

$$\langle \cos\psi \mathrm{Re}\, Y^{\ell}_{m} \rangle / \langle \mathrm{Re}\, Y^{\ell}_{m} \rangle = \frac{2\ \mathrm{Im} c}{1+|c|^2}$$

(for these moments or combinations of moments which do not contain natural parity exchange amplitudes).

A fit for c using the moments $\langle Y^{1}_{0} \rangle$, $\langle \mathrm{Re} Y^{1}_{1} \rangle$, $\langle \mathrm{Re} Y^{2}_{1} \rangle$, $\frac{1}{3}(\langle Y^{0}_{0} \rangle + \sqrt{5}\langle Y^{2}_{0} \rangle)$ and $(\langle Y^{0}_{0} \rangle - \frac{\sqrt{5}}{2}\langle Y^{2}_{0} \rangle + 3\frac{\sqrt{5}}{6}\langle Y^{2}_{2} \rangle)$ leads to the result shown in fig.8a (as function of $m_{\pi\pi}$) and in fig.8b (as function of $|t|$). The smallest nonflip amplitude is obtained for pure imaginary c. In that case the minimum "A_1" exchange (unnatural spin parity exchange nucleon nonflip) amplitudes are around 20% of the corresponding flip amplitudes.

Amplitude analysis

For the case of s and p waves the system of equations (Table 1) connecting "transversity" (f and g) amplitudes can be solved analytically. One has 15 equations (measured moments) and 14 unknowns (8 amplitudes and 6 relative phases).

Suitable addition or subtraction leads to the following subsets of equations:

$$\left.\begin{aligned}
|g_s|^2 + 3|g_0|^2 &= \sqrt{\pi}\{(t^0_0 + p^0_0) + \sqrt{5}(t^2_0 + p^2_0)\} \\
|g_0|^2 - |g_u|^2 &= \frac{\sqrt{5\pi}}{2}\{(t^2_0 + p^2_0) - \frac{1}{\sqrt{6}}(t^2_2 + p^2_2)\} \\
|g_0||g_s|\cos\gamma_{s0} &= \frac{1}{2}\sqrt{\pi}\,(t^1_0 + p^1_0) \\
|g_u||g_s|\cos\gamma_{us} &= \frac{1}{2}\sqrt{\frac{\pi}{2}}\,(t^1_1 + p^1_1) \\
|g_u||g_0|\cos\gamma_{u0} &= \frac{1}{2}\sqrt{\frac{5\pi}{6}}\,(t^2_1 + p^2_1)
\end{aligned}\right\}\quad \text{I}$$

$$\left.\begin{aligned}
|h_s|^2 + 3|h_0|^2 &= \sqrt{\pi}\{(t^0_0 - p^0_0) + \sqrt{5}(t^2_0 - p^2_0)\} \\
|h_0|^2 - |h_u|^2 &= \frac{1}{2}\sqrt{5\pi}\{(t^2_0 - p^2_0) - \frac{1}{\sqrt{6}}(t^2_2 - p^2_2)\} \\
|h_0||h_s|\cos\chi_{s0} &= \frac{1}{2}\sqrt{\pi}\,(t^1_0 - p^1_0) \\
|h_u||h_s|\cos\chi_{us} &= \frac{1}{2}\sqrt{\frac{\pi}{2}}\,(t^1_1 - p^1_1) \\
|h_u||h_0|\cos\chi_{u0} &= \frac{1}{2}\sqrt{\frac{5\pi}{6}}\,(t^2_1 - p^2_1)
\end{aligned}\right\}\quad \text{II}$$

$$\left.\begin{aligned}
|g_u|^2 - |h_N|^2 &= \sqrt{\frac{5\pi}{6}}\,(t^2_2 + p^2_2) \\
|h_u|^2 - |g_N|^2 &= \sqrt{\frac{5\pi}{6}}\,(t^2_2 - p^2_2)
\end{aligned}\right\}\quad \text{III}$$

$$\left.\begin{aligned}
|g_N||g_s|\cos\gamma_{Ns} - |h_N||h_s|\cos\chi_{Ns} &= \sqrt{\frac{\pi}{2}}\; r^1_1 \\
|g_N||g_0|\cos\gamma_{N0} - |h_N||h_0|\cos\chi_{N0} &= \sqrt{\frac{5\pi}{6}}\; r^2_1 \\
|g_u||g_N|\cos\gamma_{uN} - |h_u||h_N|\cos\chi_{uN} &= \sqrt{\frac{5\pi}{6}}\; r^2_2
\end{aligned}\right\}\quad \text{IV}$$

Solving the equation set I (set II) by substituting for the relative phase $\gamma_{us} = \gamma_{u0} - \gamma_{s0}$ one obtains a cubic equation for $|g_u|^2$ ($|h_u|^2$) with at most two physical solutions for the set $|g_u|, |g_s|, |g_0|, \gamma_{s0}, \gamma_{u0}$ ($|h_u|, |h_s|, |h_0| \chi_{s0}, \chi_{u0}$). The possible sign change of all phases γ (χ) is not counted as a separate solution.

Equation set III gives $|h_N|$ and $|g_N|$ and set IV serves to find the 2 remaining relative phases γ_{N0} and χ_{N0}.

In the amplitude analysis of the data the analytic solutions were taken as starting values for a χ^2 minimalization program fitting the measured moments by those calculated from the amplitudes according to the formulas in Table 1. In most cases all analytic solutions converged to one unique result, for the magnitude of the amplitudes. The question of phase ambiguities is still under consideration.

The t-dependence of the amplitudes for the ρ-region is shown in fig.9.

Due to the missing phase between the set of g and the set of h amplitudes the flip and nonflip amplitudes cannot be reconstructed uniquely. However the sum of intensities

$$|n|^2 + |f|^2 = |g|^2 + |h|^2$$

can be found for each partial wave separately (fig.10). Therefore also the amount of natural parity exchange can be determined exactly. In the hydrogen experiment only a lower limit for the unnatural parity exchange could be derived. Similarly a lower limit for the nonflip amplitude

$$|n| > \frac{||g| - |h||}{\sqrt{2}}$$

can be obtained.

MODEL FIT

We fit the t-dependence of the moments $\langle Y_\ell^m \rangle$, $\langle Y_\ell^m \cos\psi \rangle$, $\langle Y_\ell^m \sin\psi \rangle$ $\ell \leq 2$, $m \leq 2$ in 13 t-bins in the range $0 \leq |t| \leq 1$ GeV², in the mass region of the ρ-meson $710 \leq M_{\pi\pi} \leq 830$ MeV.

We use the simplest possible model, containing the well-known amplitudes of the "poor man's absorption"[3,5,8]) model. In order to describe the polarization measurements we add terms for A_1- and A_2-exchange.

We define the amplitudes in the t-channel helicity frame for the ππ-helicity, however the s-channel helicity is used for the nucleon helicities.

We write

$$N_0^0 = \left(\frac{\sqrt{-t_M}}{M_\pi^2 - t} e^{b_0 t} + \gamma_0 e^{b_1 t} \right) A_0$$

$$F_0^0 = \frac{\sqrt{-t'}}{M_\pi^2 - t} e^{b_0 t} \cdot A_0$$

$$N_0^1 = \left(\frac{\sqrt{-t_M}}{M_\pi^2 - t} e^{b_0 t} + \gamma_0 e^{b_1 t} \right) A_1$$

$$F_0^1 = \frac{\sqrt{-t'}}{M_\pi^2 - t} e^{b_0 t} \cdot A_1$$

$$F_1^1 = \frac{-C_A}{M_{\pi\pi}} e^{b_- t} \sqrt{2} \cdot A_1 - g_{FL}$$

$$N_{-1}^1 = N_1^1 = + g_{NF}$$

$$F_{-1}^1 = -g_{FL}$$

(t_m minimum $|t|$, $t' = t - t_M$)

A_ℓ described the ππ interaction using the phase shifts δ_ℓ^I, writing

$$A_\ell = \frac{M_{\pi\pi}}{\sqrt{q}} \sqrt{2\ell+1} \cdot T_\ell$$

decomposed into isospin

$$T_\ell = \begin{cases} \frac{2}{3} T_\ell^0 + \frac{1}{3} T_\ell^2 & \ell \text{ even} \\ T_\ell^1 & \ell \text{ odd} \end{cases}$$

and

$$T_\ell^I = e^{i\delta_\ell^I} \sin\delta_\ell^I .$$

The amplitudes $g_{F\ell}$, g_{NF} describe the A_2-exchange

$$g_{NF} = C_{NF} \; e^{b_2 t} \; e^{i\phi} \frac{\sqrt{-t'}}{\sqrt{2}} \; A_1$$

$$g_{FL} = C_{F\ell} \; e^{b_3 t} \; e^{i\phi} \frac{(-t')}{\sqrt{2}} \; A_1$$

We assume that A_1 exchange contributes only to the m = 0 nonflip amplitudes N_0^0, N_0^1 and parametrize it as $\gamma_0 e^{b_1 t}$.

We take the I=2 phase shift from reference[5]. In the ρ-region the I=0 S-wave phase was set to 90°, one global P-wave phase shift was fitted for the whole mass region.

In the simple version used so far we put $b_0 = b_1 = b_-$. The phase ϕ was assumed to be independent of t. For the fitted parameters we obtain (statistical errors only)

$$b_- = b_0 = b_{A1} = (4.33 \pm 0.02) \; \text{GeV}^{-2}$$

$$C_A = 1.12 \pm 0.01$$

$$\gamma_0 = (0.97 \pm 0.04) + i(0.712 \pm 0.02)\text{GeV}^{-1}$$

$$C_{NF} = (0.65 \pm 0.07)\text{GeV}^{-2}$$

$$C_{F\ell} = (-6.3 \pm 0.1) \; \text{GeV}^{-3}$$

$$b_{ANF} = (2.49 \pm 0.35)\text{GeV}^{-2}$$

$$b_{AFL} = (3.11 \pm 0.05)\text{GeV}^{-2}$$

$$\phi = (1.18 \pm 0.02)\text{rad.}$$

In fig.9 we show the fitted curves together with the transversity amplitudes obtained in the preceding section. Considering the simplicity of the model the agreement is satisfactory.

CONCLUSIONS

We have presented this paper to show that nucleon polarization experiments of exclusive three and more body final state reactions are feasible and can lead to unexpected results. In particular the strong nucleon polarization effect in the kinematic region which was supposed to be dominated by one pion exchange is completely unexpected. If it is due to the exchange of an additional particle this object has the quantum number of the A_1. This interpretation should be taken with caution however as it is also possible that the polarization - as is similarly true for the $\langle ReY_1^{\ell}\rangle$ moments in the hydrogen data - are the result of final state interaction.

We hope that continuation of this unfinished analysis will give an answer to this question. The importance of the problem particularly in view of the π-π phase shift analysis cannot be overemphasized.

REFERENCES

1) G. Grayer, B. Hyams, C. Jones, P. Schlein, P. Weilhammer, W. Blum, H. Dietl, W. Koch, E. Lorenz, G. Lütjens, W. Männer, J. Meissburger, W. Ochs and U. Stierlin, Nucl. Phys. B75, (1974) 189.

2) D.S. Ayres, R. Diebold, A.F. Greene, S.L. Kramer, A.J. Pawlicki and A.B. Wicklund, Proc. Int. Conf. on $\pi\pi$ scattering and associated topics, Florida State Univ., Tallahassee, 1973 (AIP Conf. Proc. no.13, particles and fields subseries no.5)p.284.

3) W. Ochs, Thesis, Ludwig-Maximilians-Universität, Munich (1973); and

B. Hyams, C. Jones, P. Weilhammer, W. Blum, H. Dietl, G. Grayer, W. Koch, E. Lorenz, G. Lütjens, J. Meissburger, W. Ochs, U. Stierlin, and F. Wagner, Proc. Int. Conf. on $\pi\pi$ scattering and associated topics, Florida State Univ., Tallahassee, 1973 (AIP Conf. Proc. no.13, particles and fields subseries no.5)p.206; Nucl. Phys. B64, (1973) 134.

4) P. Estabrooks and A.D. Martin, Phys. Letters 53B, (1974) 253.

5) B. Hyams, C. Jones, P. Weilhammer, W. Blum, H. Dietl, G. Grayer, W. Koch, E. Lorenz, G. Lütjens, W. Männer, J. Meissburger, W. Ochs and U. Stierlin, Nucl. Phys. B100, (1975) 205.

6) B. Hyams, C. Jones, P. Weilhammer, W. Blum, H. Dietl, G. Grayer, E. Lorenz, G. Lütjens, W. Männer, J. Meissburger, W. Ochs and U. Stierlin, Phys. Letters 51B, (1974) 272.

7) G. Grayer, B. Hyams, C. Jones, P. Weilhammer, W. Blum, H. Dietl, W. Koch, E. Lorenz, G. Lütjens, W. Männer, J. Meissburger, W. Ochs and U. Stierlin, Nucl. Physics B50, (1972) 29.

8) P.K. Williams, Phys. Rev. D1, (1970) 1312.

Relations between moments and amplitudes

	"helicity amplitudes" non spin flip $n_s \equiv n^0_0 \; n_0 \equiv {}^u n^1_0 \; n_u \equiv {}^u n^1_1 \; n_N \equiv {}^N n^1_1$ spin flip $f_s \equiv f^0_0 \; f_0 \equiv {}^u f^1_0 \; f_u \equiv {}^u f^1_1 \; f_N \equiv {}^N f^1_1$	"transversity amplitudes" Recoil transversity up $g_s \equiv g^0_0 \; g_0 \equiv {}^u g^1_0 \; g_u \equiv {}^u g^1_1 \; h_N \equiv {}^N h^1_1$ Recoil transversity down $h_s \equiv h^0_0 \; h_0 \equiv {}^u h^1_0 \; h_u \equiv {}^u h^1_1 \; g_N \equiv {}^N g^1_1$
$t^0_0 = \langle Y^0_0 \rangle$	$\frac{1}{\sqrt{4\pi}}\{\lvert n_s\rvert^2+\lvert f_s\rvert^2+\lvert n_0\rvert^2+\lvert f_0\rvert^2+ \lvert n_u\rvert^2+\lvert f_u\rvert^2+\lvert n_N\rvert^2+\lvert f_N\rvert^2$	$\frac{1}{\sqrt{4\pi}}\{\lvert g_s\rvert^2+\lvert h_s\rvert^2+\lvert g_0\rvert^2+\lvert h_0\rvert^2+ \lvert g_u\rvert^2+\lvert h_u\rvert^2+\lvert g_N\rvert^2+\lvert h_N\rvert^2\}$
$t^1_0 = \langle Y^1_0 \rangle$	$\frac{1}{\sqrt{\pi}} \mathrm{Re}\{n_0 n^*_s + f_0 f^*_s\}$	$\frac{1}{\sqrt{\pi}} \{g_0 g^*_s + h_0 h^*_s\}$
$t^1_1 = 2\langle \mathrm{Re}Y^1_1 \rangle$	$\sqrt{\frac{2}{\pi}} \mathrm{Re}\{n_u n^*_s + f_u f^*_s\}$	$\sqrt{\frac{2}{\pi}} \mathrm{Re}\{g_u g^*_s + h_u h^*_s\}$
$t^2_0 = \langle Y^2_0 \rangle$	$\frac{1}{\sqrt{20\pi}}\{2(\lvert n_0\rvert^2+\lvert f_0\rvert^2)- \lvert n_u\rvert^2-\lvert f_u\rvert^2-\lvert n_N\rvert^2-\lvert f_N\rvert^2\}$	$\frac{1}{\sqrt{20\pi}}\{2\lvert g_0\rvert^2+2\lvert h_0\rvert^2-\lvert g_u\rvert^2-\lvert h_u\rvert^2-\lvert g_N\rvert^2-\lvert h_N\rvert^2\}$
$t^2_1 = 2\langle \mathrm{Re}Y^2_1 \rangle$	$\sqrt{\frac{6}{5\pi}} \mathrm{Re}\{n_u n^*_0 + f_u f^*_0\}$	$\sqrt{\frac{6}{5\pi}} \mathrm{Re}\{g_u g^*_0 + h_u h^*_0\}$
$t^2_2 = 2\langle \mathrm{Re}Y^2_2 \rangle$	$\sqrt{\frac{3}{10\pi}}\{\lvert n_u\rvert^2+\lvert f_u\rvert^2-\lvert n_N\rvert^2-\lvert f_N\rvert^2\}$	$\sqrt{\frac{3}{10\pi}}\{\lvert g_u\rvert^2+\lvert h_u\rvert^2-\lvert g_N\rvert^2-\lvert h_N\rvert^2\}$
$p^0_0 = 2\langle \cos\psi Y^0_0 \rangle$	$\frac{1}{\sqrt{4\pi}} 2\mathrm{Im}\{n_s f^*_s + n_0 f^*_0 + n_u f^*_u + n_N f^*_N\}$	$\frac{1}{\sqrt{4\pi}}\{\lvert g_s\rvert^2-\lvert h_s\rvert^2+\lvert g_0\rvert^2-\lvert h_0\rvert^2+ \lvert g_u\rvert^2-\lvert h_u\rvert^2-\lvert g_N\rvert^2+\lvert h_N\rvert^2\}$
$p^1_0 = 2\langle \cos\psi Y^1_0 \rangle$	$\frac{1}{\sqrt{\pi}} \mathrm{Im}\{n_0 f^*_s - f_0 n^*_s\}$	$\frac{1}{\sqrt{\pi}} \mathrm{Re}\{g_0 g^*_s - h_0 h^*_s\}$
$p^1_1 = 4\langle \cos\psi \mathrm{Re}Y^1_1 \rangle$	$\sqrt{\frac{2}{\pi}} \mathrm{Im}\{n_u f^*_s - f_u n^*_s\}$	$\sqrt{\frac{2}{\pi}} \mathrm{Re}\{g_u g^*_s - h_u h^*_s\}$
$p^2_0 = 2\langle \cos\psi Y^2_0 \rangle$	$\frac{1}{\sqrt{20\pi}} 2\mathrm{Im}\{2n_0 f^*_0 - n_u f^*_u - n_N f^*_N\}$	$\frac{1}{\sqrt{20\pi}}\{2\lvert g_0\rvert^2-2\lvert h_0\rvert^2-\lvert g_u\rvert^2+\lvert h_u\rvert^2+\lvert g_N\rvert^2-\lvert h_N\rvert^2\}$
$p^2_1 = 4\langle \cos\psi \mathrm{Re}Y^2_1 \rangle$	$\sqrt{\frac{6}{5\pi}} \mathrm{Im}\{n_u f^*_0 - f_u n^*_0\}$	$\sqrt{\frac{6}{5\pi}} \mathrm{Re}\{g_u g^*_0 - h_u h^*_0\}$
$p^2_2 = 4\langle \cos\psi \mathrm{Re}Y^2_2 \rangle$	$\sqrt{\frac{3}{10\pi}} 2\mathrm{Im}\{n_u f^*_u - n_N f^*_N\}$	$\sqrt{\frac{3}{10\pi}}\{\lvert g_u\rvert^2-\lvert h_u\rvert^2+\lvert g_N\rvert^2-\lvert h_N\rvert^2\}$
$r^1_1 = 4\langle \sin\psi \mathrm{Im}Y^1_1 \rangle$	$-\sqrt{\frac{2}{\pi}} \mathrm{Im}\{n_N f^*_s + f_N n^*_s\}$	$-\sqrt{\frac{2}{\pi}} \mathrm{Re}\{g_N g^*_s - h_N h^*_s\}$
$r^2_1 = 4\langle \sin\psi \mathrm{Im}Y^2_1 \rangle$	$-\sqrt{\frac{6}{5\pi}} \mathrm{Im}\{n_N f^*_0 + f_N n^*_0\}$	$-\sqrt{\frac{6}{5\pi}} \mathrm{Re}\{g_N g^*_0 - h_N h^*_0\}$
$r^2_2 = 4\langle \sin\psi \mathrm{Im}Y^2_2 \rangle$	$-\sqrt{\frac{6}{5\pi}} \mathrm{Im}\{n_N f^*_u + f_N n^*_u\}$	$-\sqrt{\frac{6}{5\pi}} \mathrm{Re}\{g_N g^*_u - h_N h^*_u\}$

Figure captions

Fig. 1 : Definition of kinematic quantities. ψ angle between normal to production plane and (transverse) polarization of the protons taken in the rest frame of the proton, θ, ϕ polar and azimuthal angle of the π^- in the rest frame of the $\pi\pi$ system. (θ=0 corresponds to the opposite direction of the neutron in the t-channel system and to the beam direction in the s-channel system).

Fig. 2 : Schematic view of the apparatus: C Cerenkov counters, S scintillation counters, W spark chambers, M magnets, T target.

Fig. 3 : Square of Missing Mass of a random sample of data calculated under the assumption that the process occurs on free hydrogen
a) for the butanol (+) and the hydrogen (×) target
b) for low ($t < 0.01$)(+) and high ($0.2 < t$)(×) four momentum **transfer** on the butanol.

Fig. 4 : Distribution of events in the angle ψ before correcting for the acceptance of the spectrometer for positive, (+) and for negative (×) polarization direction.
If no nucleon polarization were present the two distributions should be identical.

Fig. 5 : Mass spectrum and normalized moments $\langle ReY_0^\ell \rangle$ for
a) Butanol
b) Hydrogen

Fig. 6 : Unnormalized moments $\frac{d\sigma}{dmdt} \langle Y_0^\ell \rangle$ and $\frac{d\sigma}{dmdt} \langle \cos\psi Y_0^\ell \rangle$. Combined results from hydrogen and butanol experiments.

Fig. 7 : Cross section $\frac{d\sigma}{dt}$ and normalized moments $\langle Y_0^\ell \rangle$ and $\langle \cos\psi Y_0^\ell \rangle$ for the ρ-mass region ($0.71 < m_{\pi\pi} < 0.83$).

Fig. 8 : Ratio between nonflip and flip amplitudes ($n = c \cdot f$). Results of a fit of $\frac{2 Im c}{1+|c|^2}$ by the ratio of moments
a) as function of $m_{\pi\pi}$ for $0.01 < t < 0.2$
b) as function of t for $0.71 < m < 0.83$.

Fig. 9 : t-dependence of nucleon "transversity" amplitudes in the ρ region ($0.71 < m_{\pi\pi} < 0.83$). The amplitudes have been obtained by a 1-constraint fit to the moments $\langle ReY_m^\ell \rangle$, $\langle \cos\psi ReY_m^\ell \rangle$ and $\langle \sin\psi ImY_m^\ell \rangle$ with $\ell < 2$.

Fig. 10 : Intensities of the partial waves calculated from the transversity amplitudes.

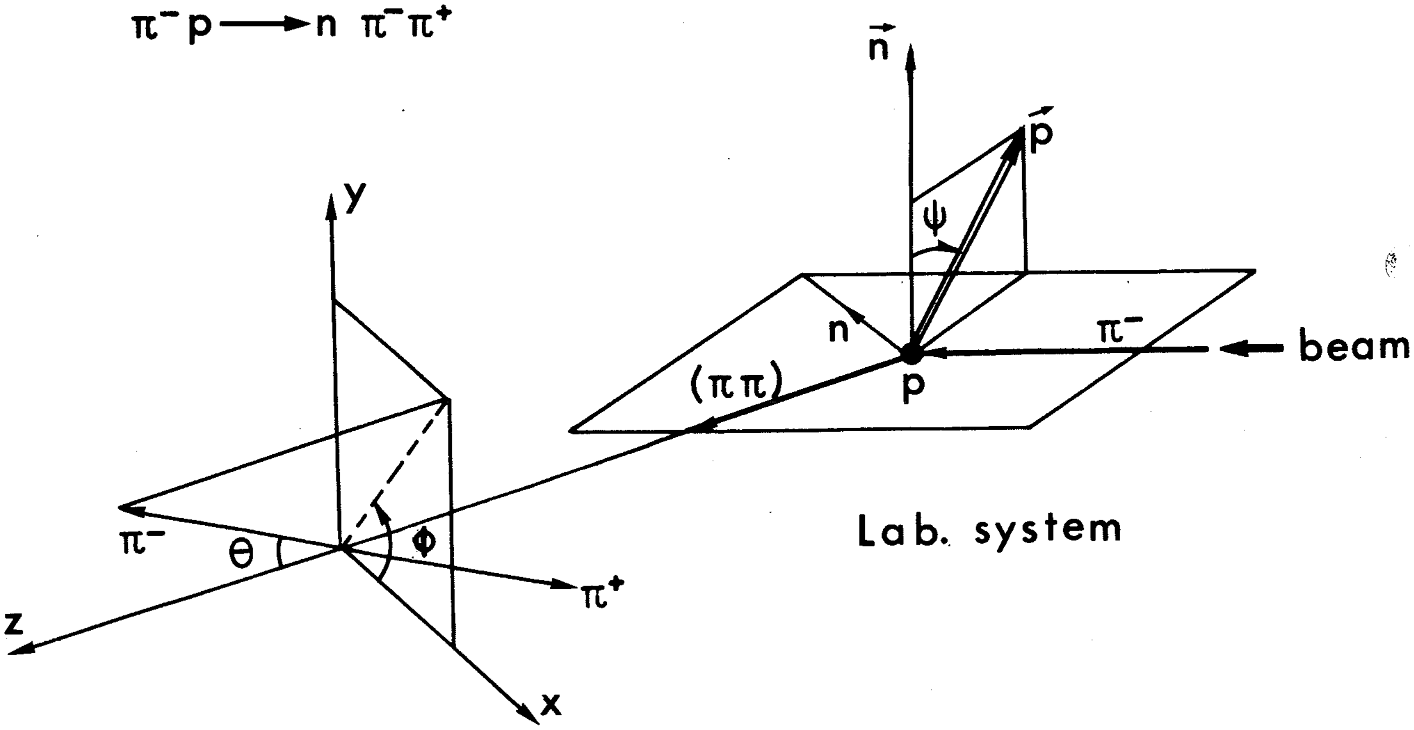

rest system of $(\pi\pi)$

Fig.1

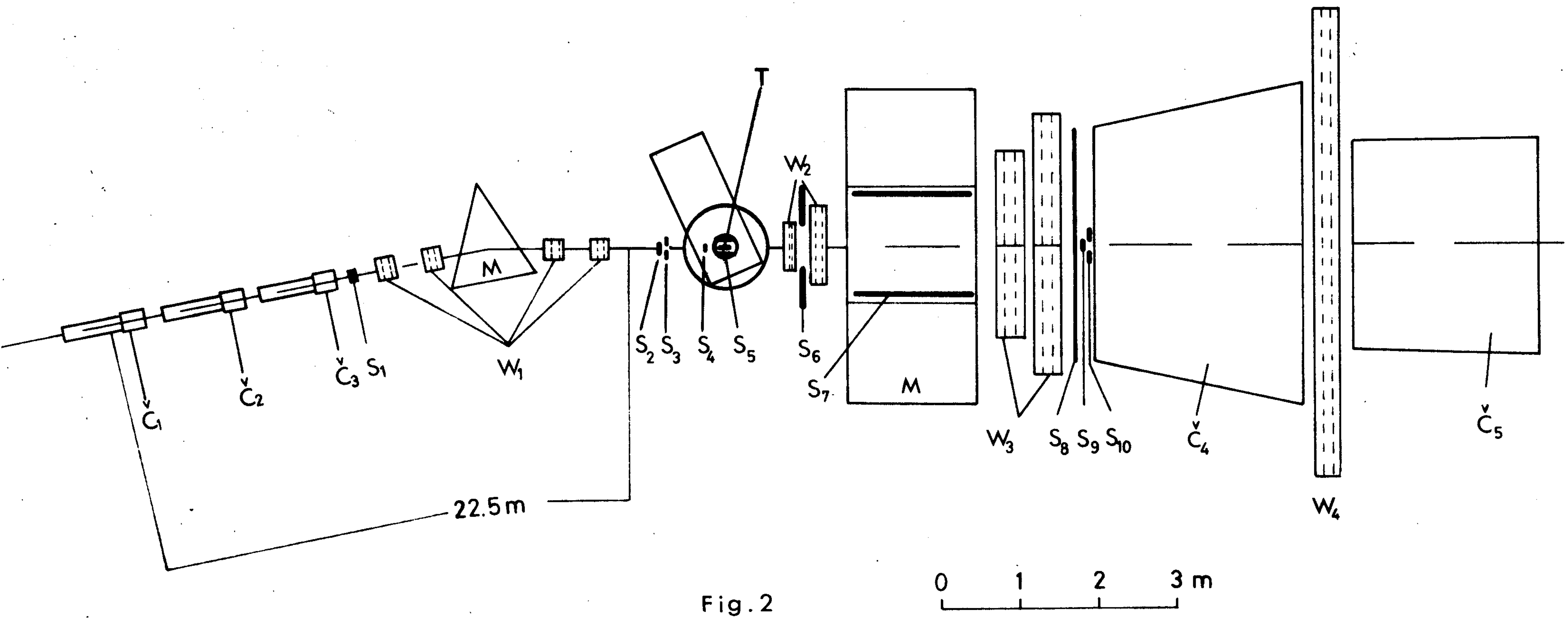

Č1
Č2
Č3
S1
W1
M
22.5 m
S2 S3
S4
S5
T
W2
S6
S7
M
W3
S8 S9 S10
Č4
W4
Č5
0 1 2 3 m

Fig. 2

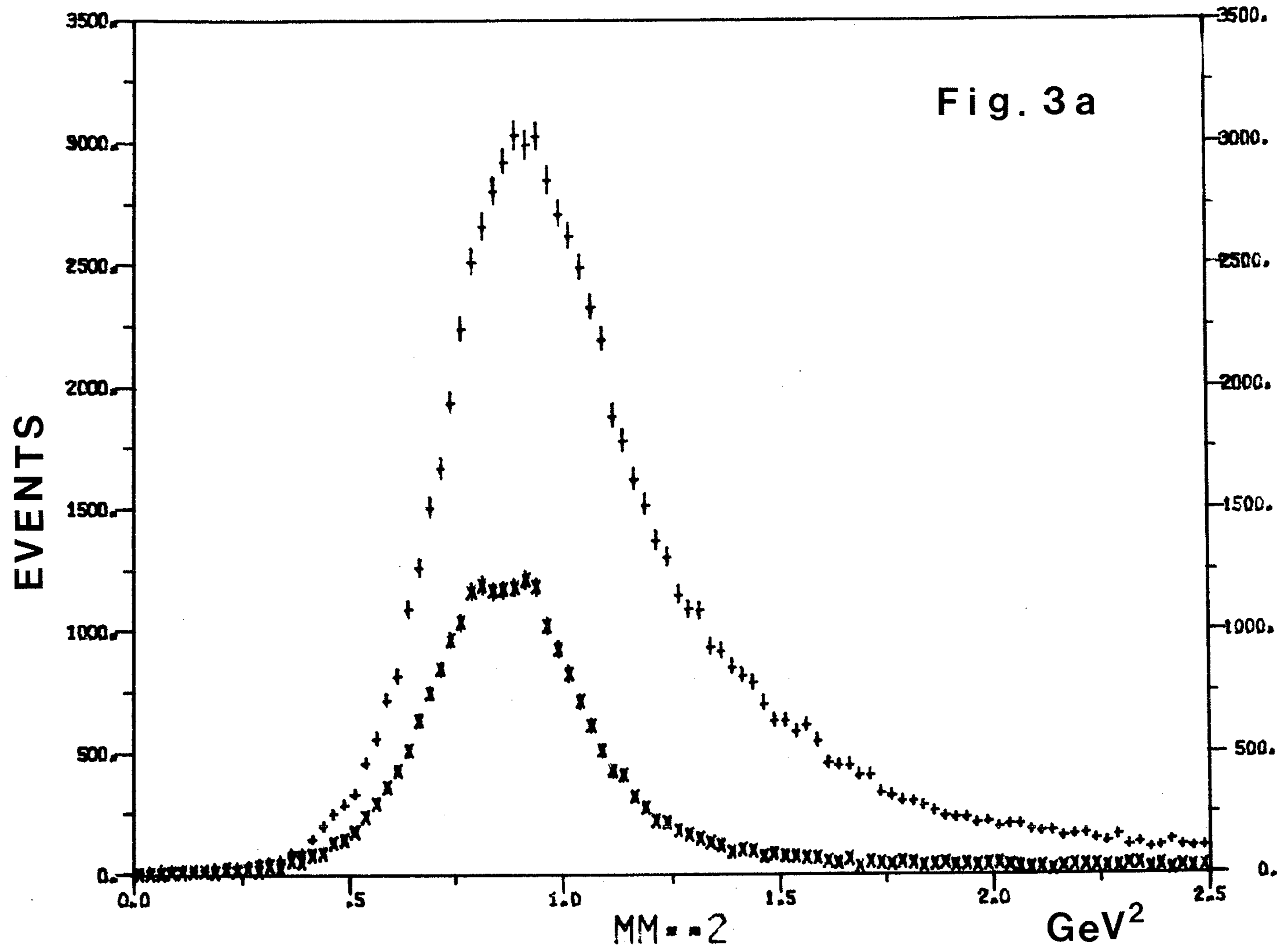
Fig. 3a
EVENTS
MM**2
GeV^2

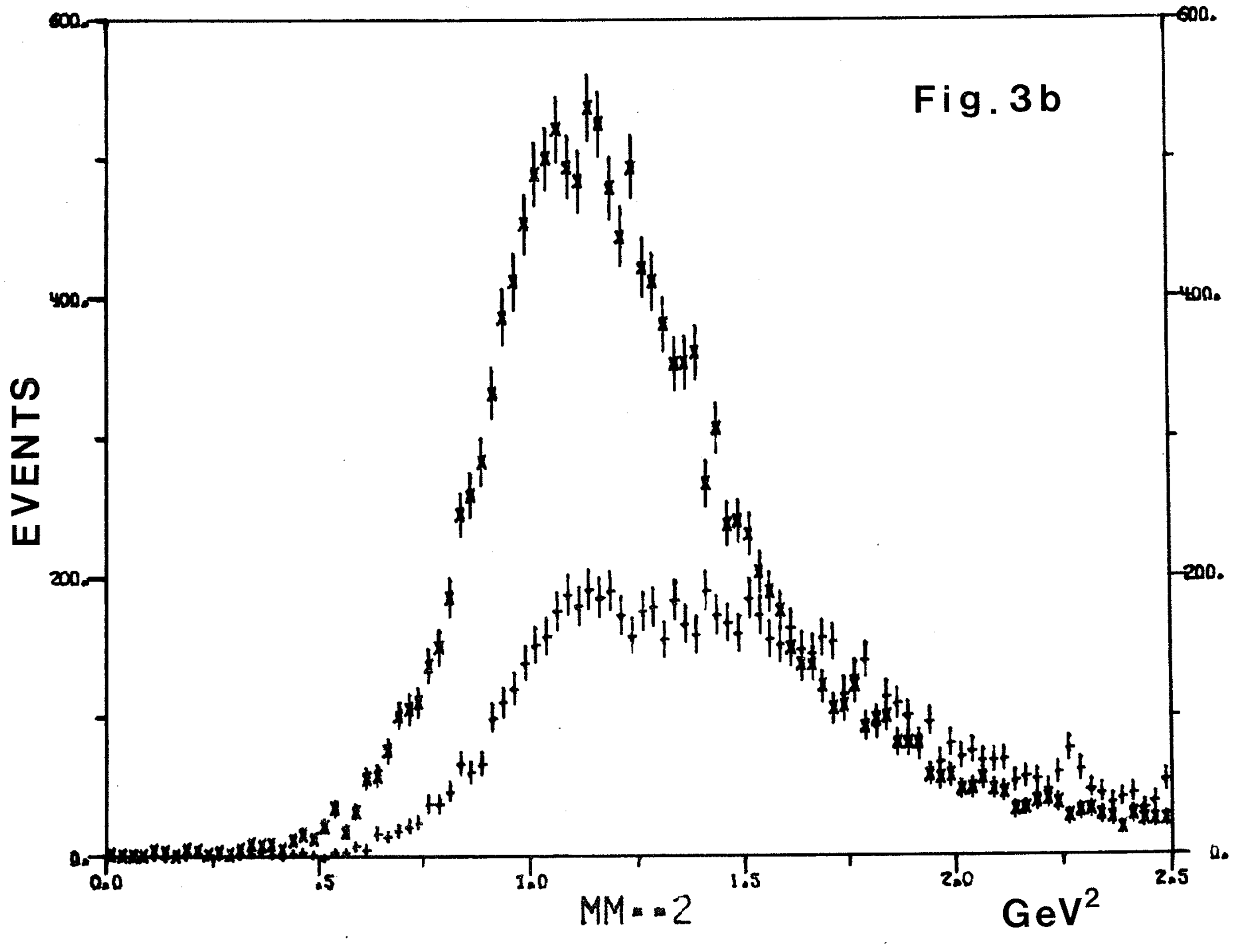
Fig. 3b
EVENTS
MM**2
GeV^2

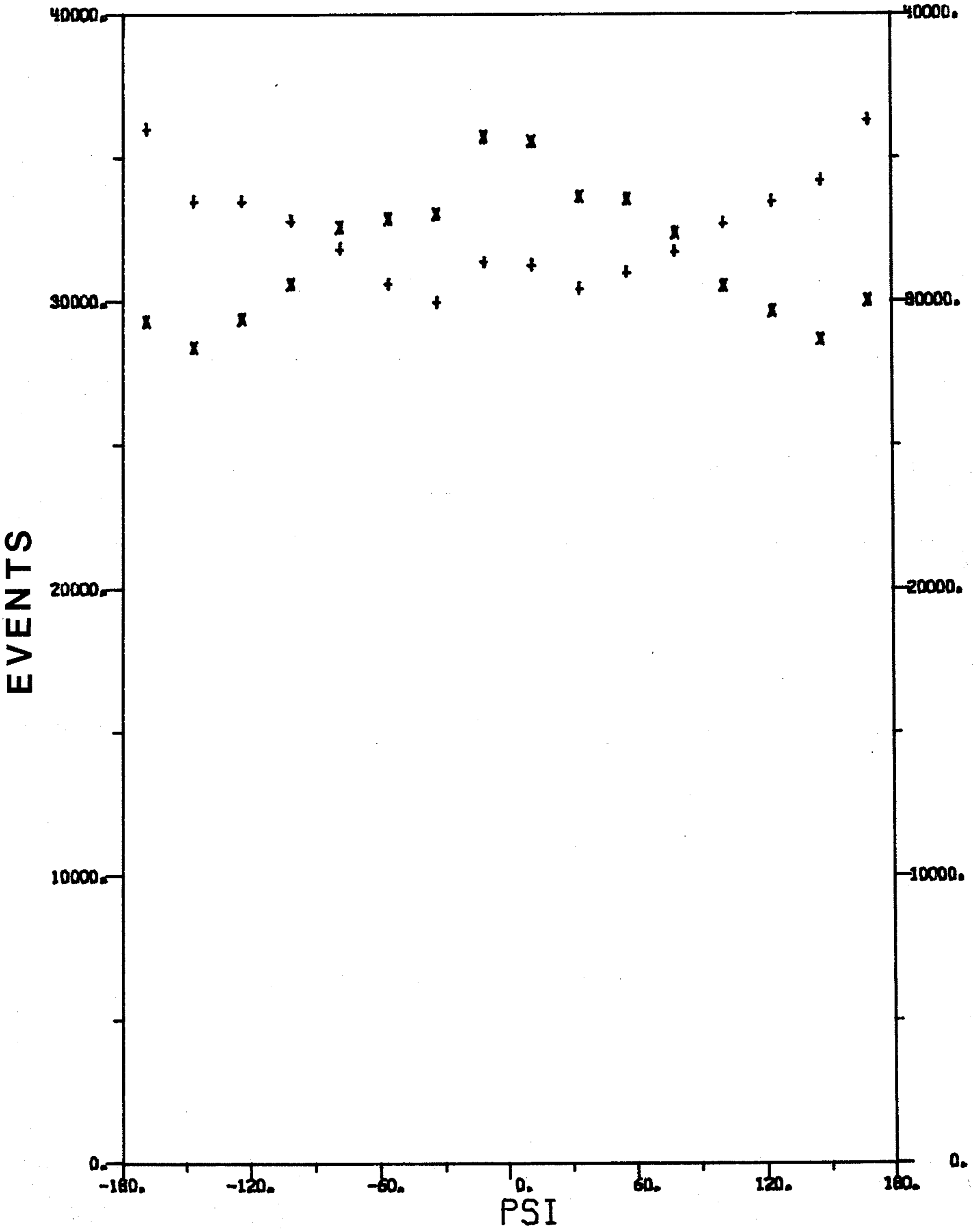
40000.
30000.
20000.
10000.
0.
40000.
30000.
20000.
10000.
0.
EVENTS
-180.
-120.
-60.
0.
60.
120.
180.
PSI

Fig. 4

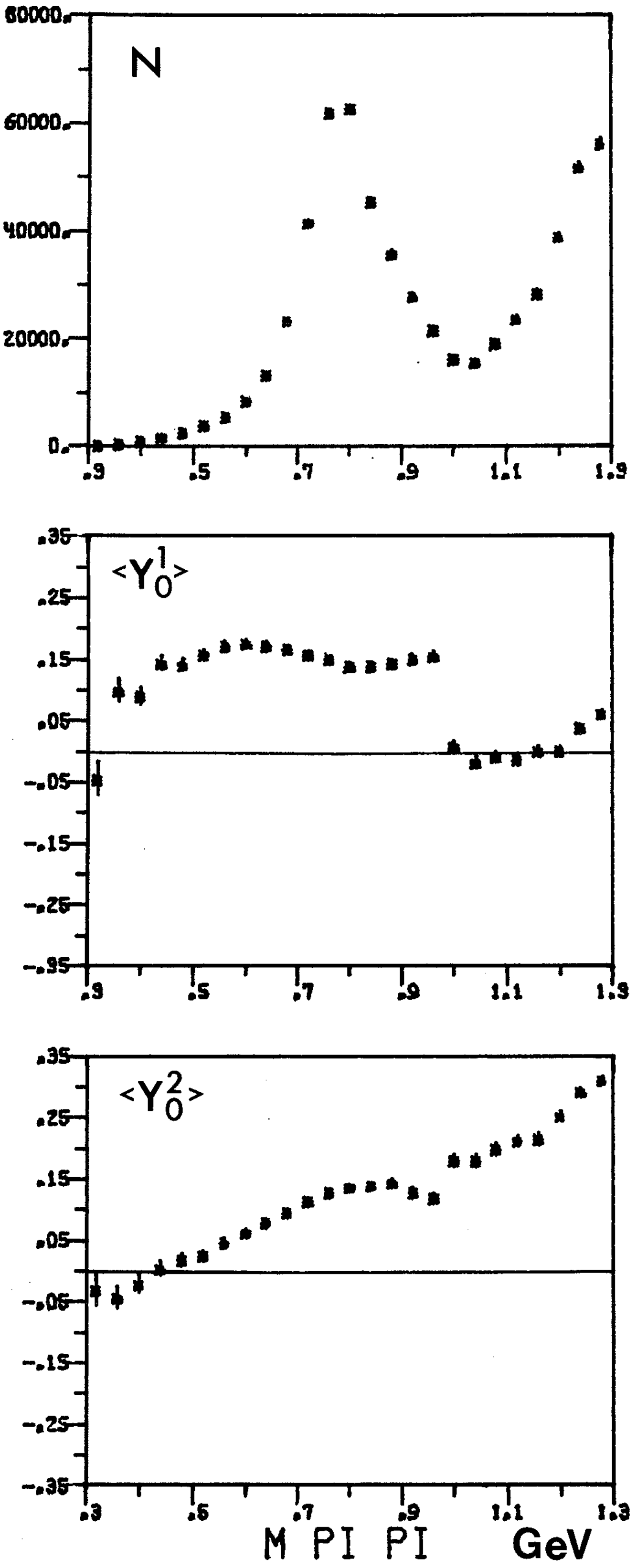
N
80000.
60000.
40000.
20000.
0.
<Y10>
<Y20>
.35
.25
.15
.05
-.05
-.15
-.25
-.35
.3
.5
.7
.9
1.1
1.3
M PI PI
GeV

Fig.5a)

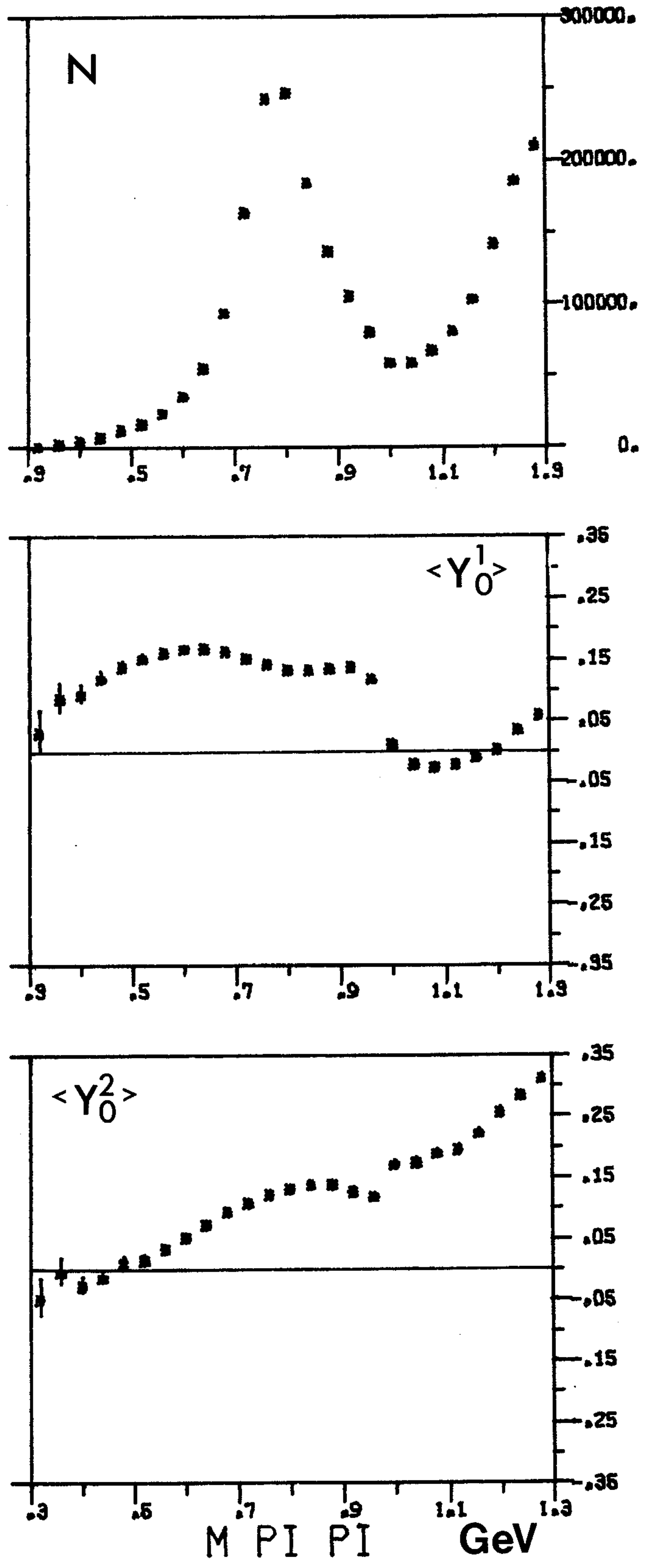
N
300000.
200000.
100000.
0.
<Y10>
<Y20>
.35
.25
.15
.05
-.05
-.15
-.25
-.35
.3
.5
.7
.9
1.1
1.3
M PI PI
GeV

Fig.5b)

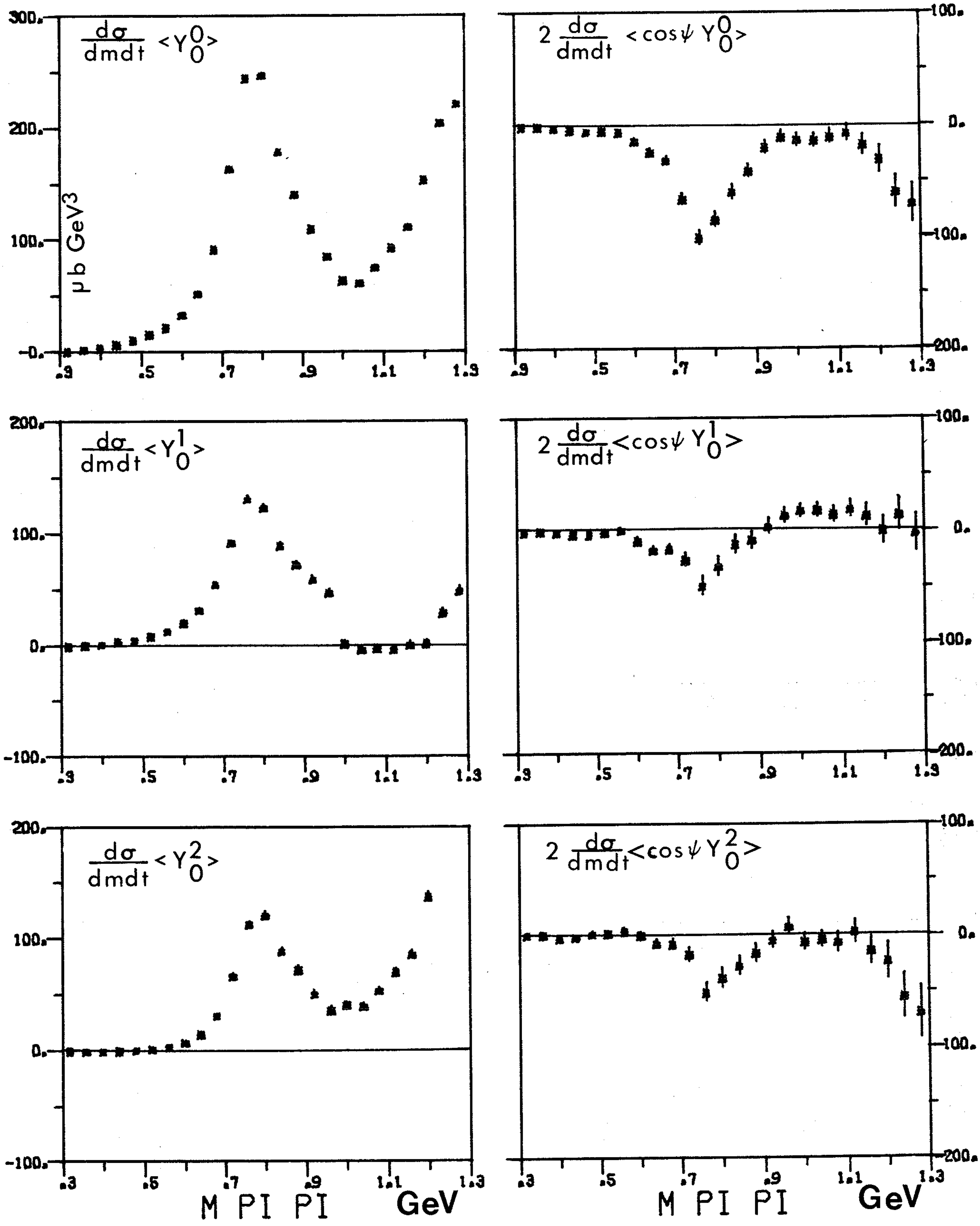

dσ/dmdt <Y^0_0>
2 dσ/dmdt <cosψ Y^0_0>
dσ/dmdt <Y^1_0>
2 dσ/dmdt <cosψ Y^1_0>
dσ/dmdt <Y^2_0>
2 dσ/dmdt <cosψ Y^2_0>
μb GeV3
M PI PI GeV
M PI PI GeV

Fig. 6

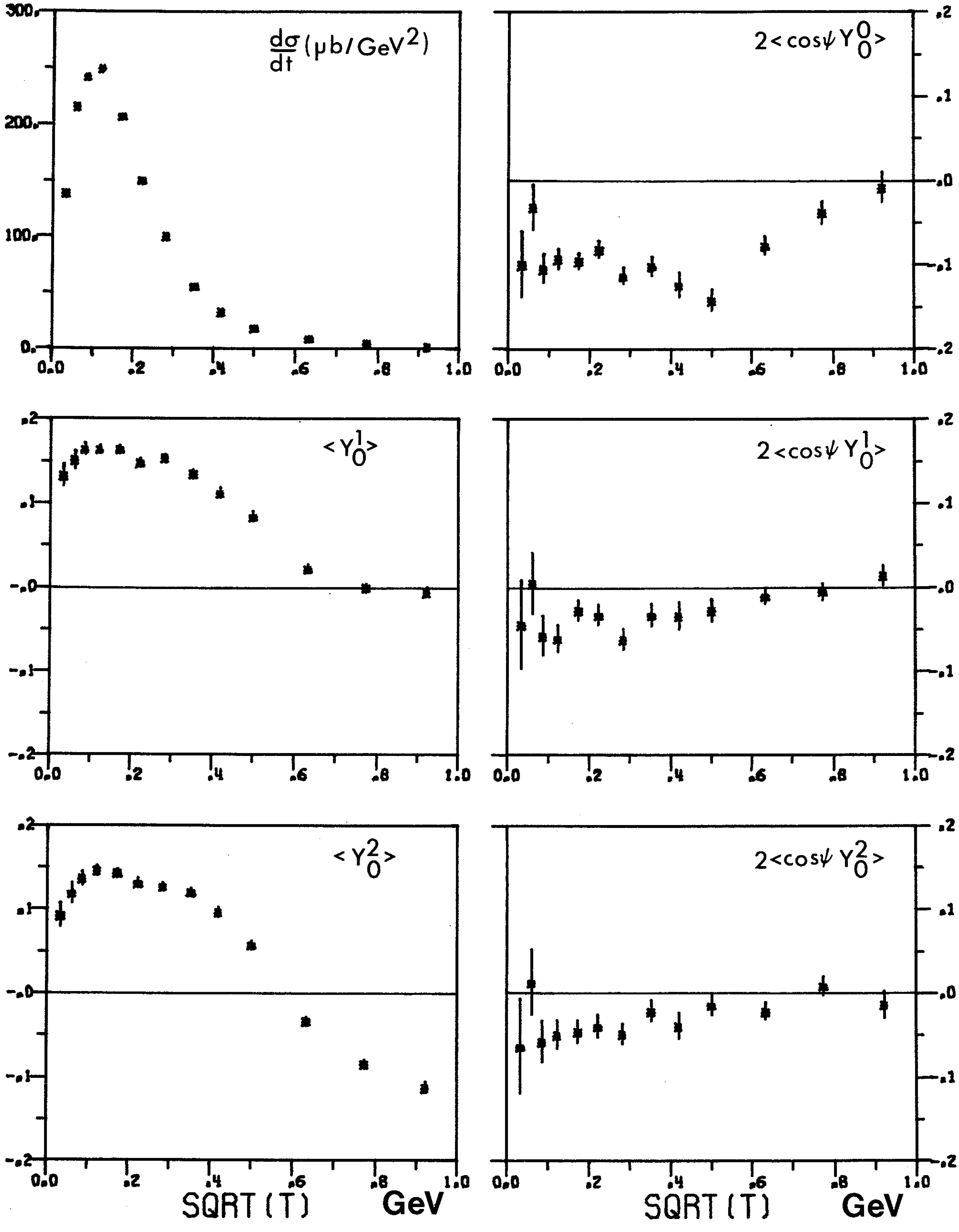
dσ/dt (μb/GeV²)
2<cosψ Y⁰₀>
<Y¹₀>
2<cosψ Y¹₀>
<Y²₀>
2<cosψ Y²₀>
SQRT(T) GeV
SQRT(T) GeV

Fig. 7

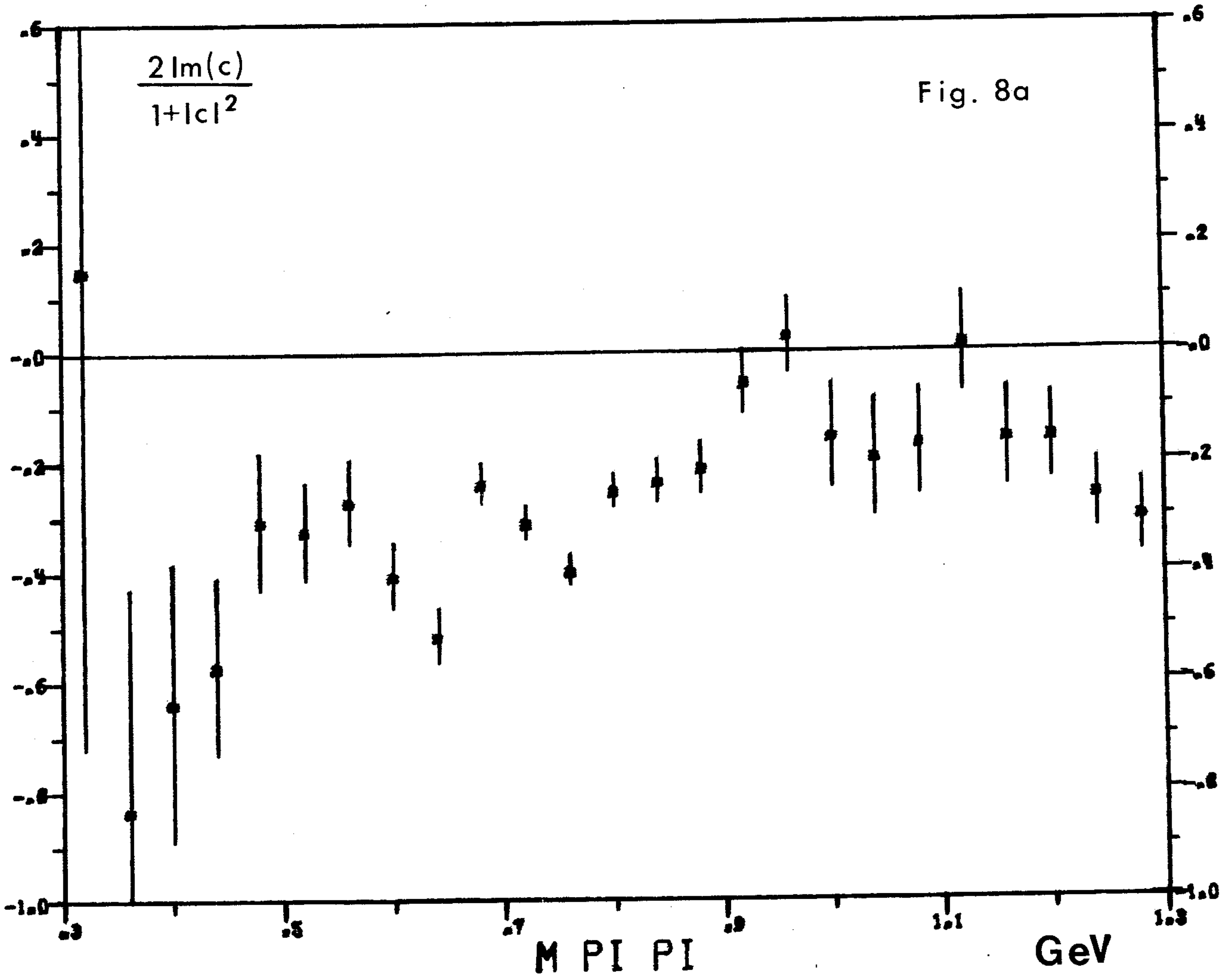
2 Im(c) / 1+|c|^2
Fig. 8a
M PI PI
GeV

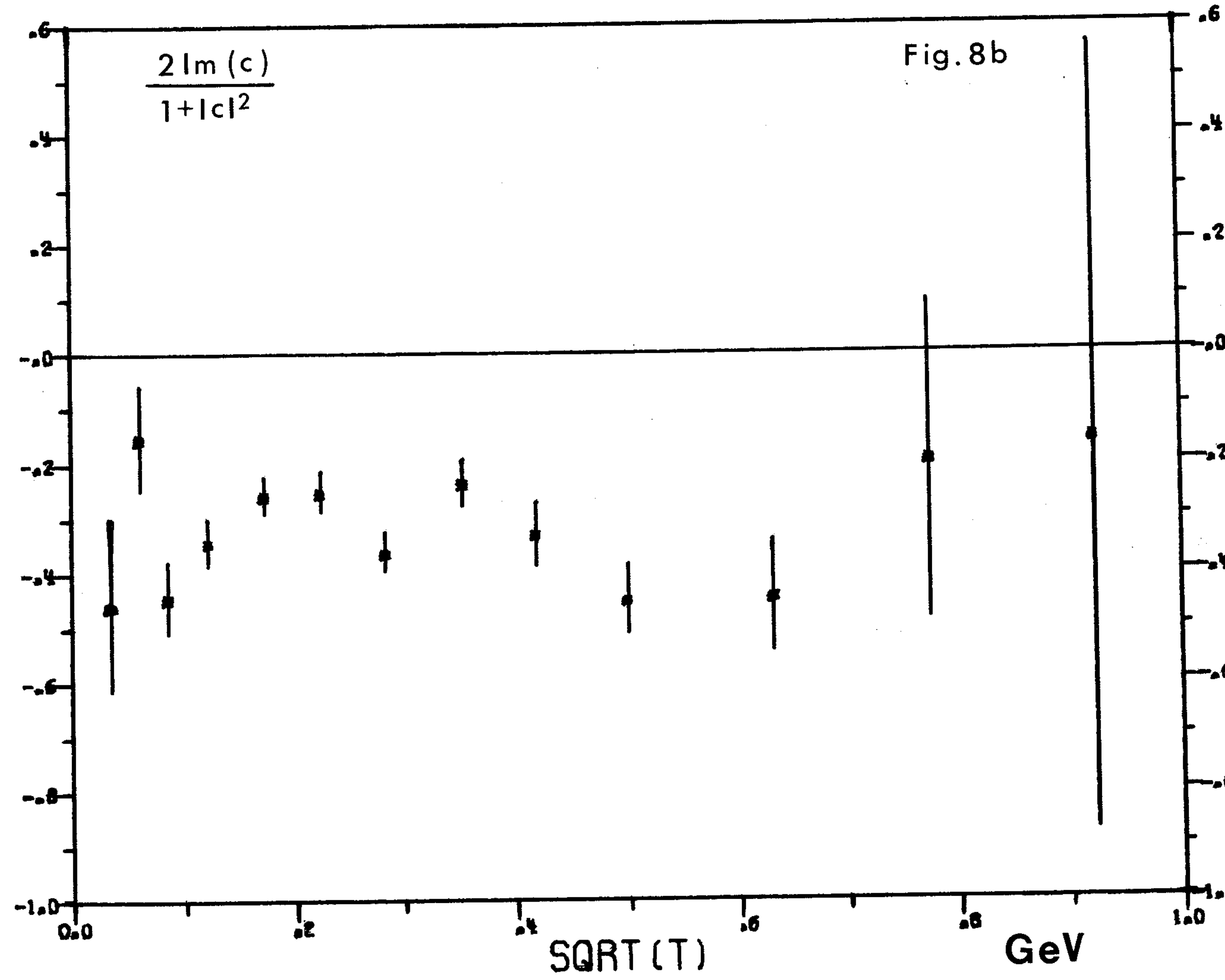
2 Im (c) / 1+|c|^2
Fig. 8b
SQRT(T)
GeV

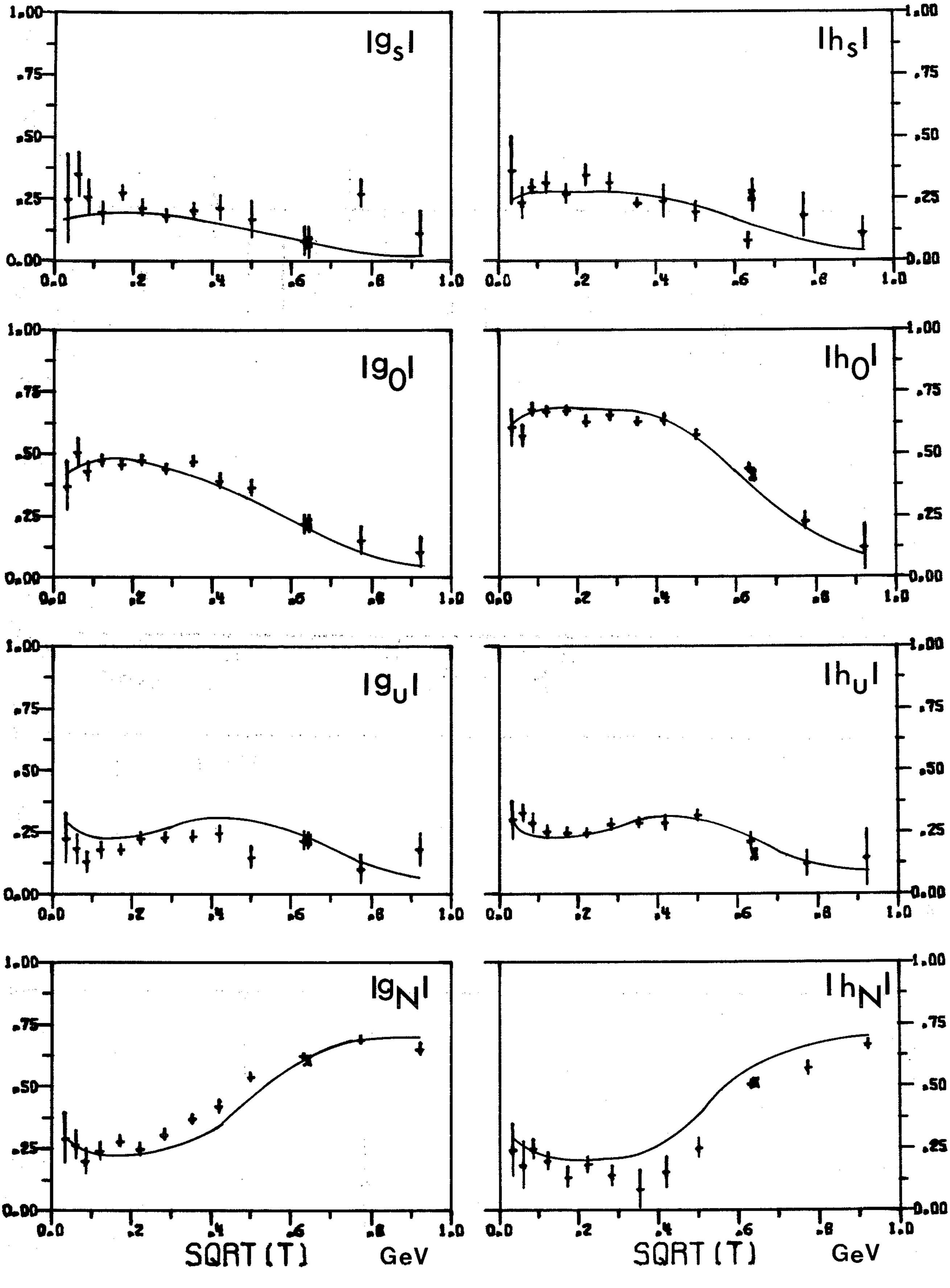

Fig. 9

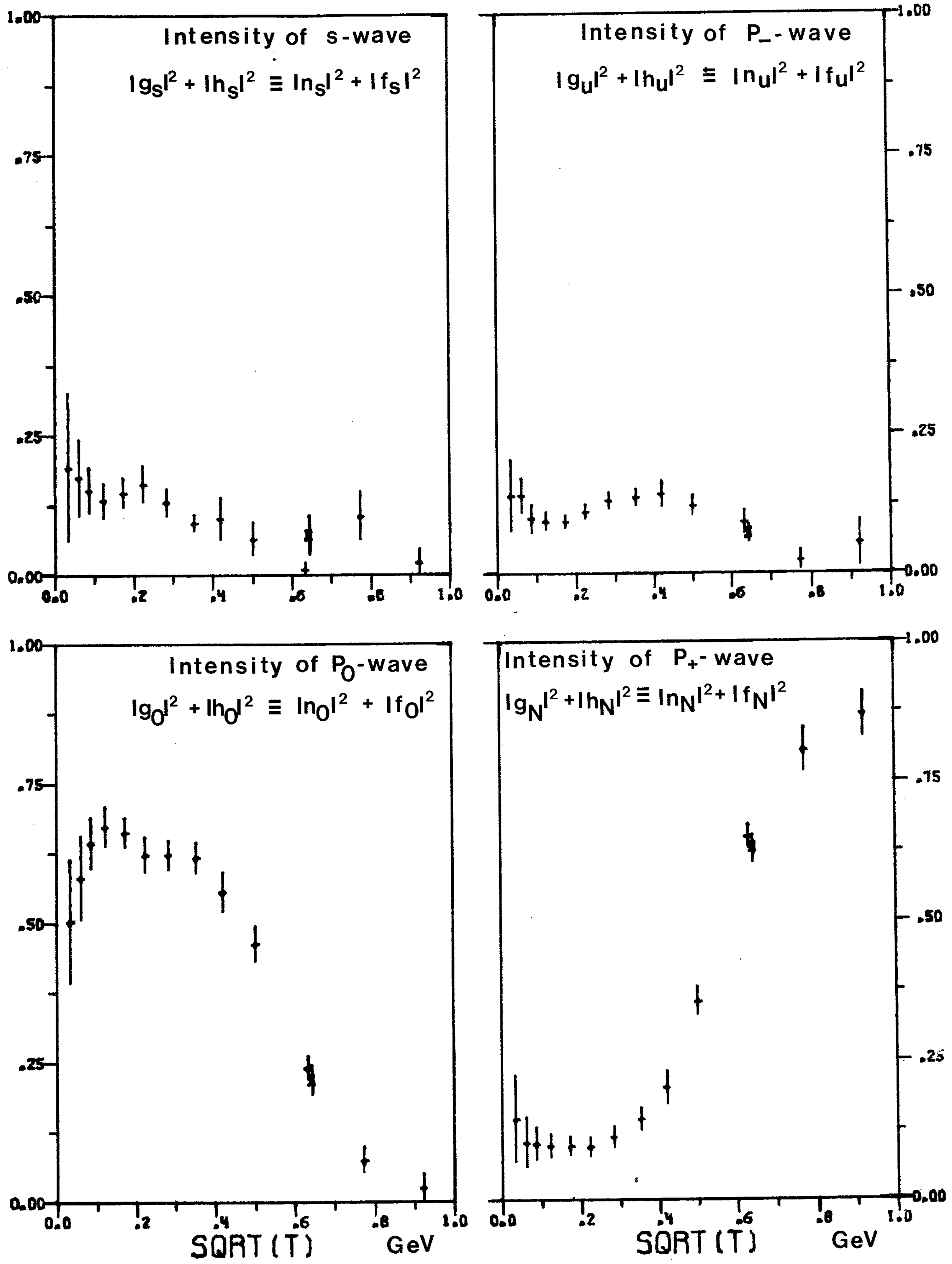

Intensity of s-wave
|gs|² + |hs|² ≡ |ns|² + |fs|²
Intensity of P₋-wave
|gu|² + |hu|² ≡ |nu|² + |fu|²
Intensity of P0-wave
|g0|² + |h0|² ≡ |n0|² + |f0|²
Intensity of P₊-wave
|gN|² + |hN|² ≡ |nN|² + |fN|²
1.00
.75
.50
.25
0.00
0.0
.2
.4
.6
.8
1.0
SQRT(T)
GeV

Fig.10